# Computation-Driven Design: Dielectric Loss Mechanism and Performance Optimization of Epoxy/Anhydride Curing System

Yi Zhang [1,a], Yunhua He [2,b], Fusheng Zhou[1,c], Yufeng Song [2,d], Jiaming Xiong[1,e], Xueting Cheng[2,f], and ChaoGao [1,g1]

[1] Electric Power Research Institute Co., Ltd., China South Power Grid, Guangzhou, China;
[2] Electric Power Research Institute of Yunnan Electric Power Grid Co., Ltd., Kunming, China.

## ABSTRACT

The dielectric loss characteristics of epoxy resin, as a critical insulating material in high-frequency transformers, are essential to the performance and safety of the transformers. This paper explores the dielectric loss mechanism of epoxy/anhydride curing systems through molecular dynamics simulations, particularly focusing on the impact of segmental motion characteristics on dielectric loss. The study reveals that the probability density distribution of the motion speeds of various segments in the epoxy/anhydride cross-linked network follows the Maxwell-Boltzmann distribution. The increased rigidity of the curing agent structure reduces the displacement capability of anhydride and ester bond segments but provides greater motion space for epoxy segments, reducing motion resistance. Additionally, the methyl side chains in the anhydride further promote the motion of epoxy segments by providing additional displacement and support. These discoveries offer crucial insights for optimizing epoxy resin design, significantly contributing to the performance enhancement of high-frequency transformers in smart grids.

**Keywords:** Epoxy resin; Epoxy/anhydride cross-linked system; Dielectric loss.

## 1. INTRODUCTION

With the development of smart grids, the application of High-Frequency Transformers (HFT) is becoming increasingly widespread[1,2]. Epoxy Resin (EP) has become an important insulating material in high-frequency transformers due to its high dielectric strength and good heat resistance[3]. High dielectric loss of epoxy resin can result in increased temperatures in high-frequency transformers, potentially leading to insulation failure and jeopardizing the safe and stable operation of the power system[4]. However, the diversity of EP and curing agent types means that traditional design methods, which are inspired by dielectric loss measurements, cannot effectively design low-dielectric-loss epoxy systems from numerous candidate EP systems[5–7]. With the development of materials informatics, material computation-driven design based on methods such as molecular dynamics has become an efficient means of designing new materials[8–10]. Therefore, researching the computationally driven design of low-dielectric-loss epoxy resins for high-frequency transformers is of great significance in reducing the risk of thermal runaway and improving transformer efficiency[11].

Previous research has found that the type of curing agent affects the dielectric loss of epoxy cured products and established molecular models of different epoxy/anhydride curing systems[12]. Molecular dynamics methods were used to analyze the differences in microscopic parameters of different epoxy/anhydride curing systems[13,14]. However, the dielectric loss of epoxy cures under high-frequency electric fields is related to the local chain segment movements[15]. Merely analyzing the microscopic characteristics of the cross-linked network structure is not enough to elucidate the motion differences of different chain segments within the curing system, and cannot quantitatively characterize the contributions of each chain segment to the dielectric loss process in epoxy cured products.

Therefore, to investigate the dielectric loss mechanism of the epoxy/anhydride curing system, the differences in the motion characteristics of different chain segments in the epoxy/anhydride curing system were studied. By deconstructing a typical epoxy/anhydride cross-linked network, the epoxy/anhydride cross-linked model was deconstructed into three parts: epoxy segments, anhydride segments, and unreacted anhydride. The velocity distribution patterns of different segments were

[1a] zhangyi3@csg.cn, [b] 95187694@qq.com, [c] zhoufs@csg.cn, [d] 972292017@qq.com, [e] xiongjm@csg.cn, [f] chengxueting@foxmail.com, [g] gaochao@csg.cn

The International Conference Optoelectronic Information and Optical Engineering (OIOE2024), edited by Yang Yue, Lu Leng, Proc. of SPIE Vol. 13513, 1351303 · © 2025 SPIE · 0277-786X · © The Authors.
 · doi: 10.1117/12.3045339

analyzed. The results indicated that the probability density distribution of segment motion rates within the epoxy/anhydride cross-linked network conforms to the Maxwell-Boltzmann distribution. Combined with the free volume fractions of each system, the displacement characteristics of different segments were analyzed. The results demonstrate that the displacement characteristics of the epoxy/anhydride cross-linked network are related to the structure of the curing agent. The increased rigidity of the curing agent's six-membered ring reduces the displacement ability of anhydride and ester bond segments but provides a "supporting" effect for the cross-linked network, thereby increasing the motion space of the epoxy segments and reducing the motion resistance of the epoxy segments. The methyl side chains in the anhydride provide additional displacement for ester bond segments on the one hand, and also provide support for the cross-linked network on the other, thereby increasing the motion space of the epoxy segments and reducing the motion resistance of the epoxy segments.

## 2. LOCAL CHAIN SEGMENT MOTION BEHAVIOR IN EPOXY/ANHYDRIDE SYSTEM

In previous work, a computational method for the local chain segment motion in epoxy/anhydride cross-linked networks has been proposed, which can identify specific local chain segments in the epoxy/anhydride cross-linked network and analyze their motion behavior. Therefore, in this work, the velocity distribution and mean square displacement of local chain segments in the epoxy/anhydride cross-linked network were quantitatively analyzed; the reasons for the differences in the motion capabilities of chain segments in the epoxy/anhydride cross-linked network were elucidated.

### 2.1 Deconstruction of Epoxy/Anhydride Cross-linked Structure

According to the curing reaction mechanism of epoxy/anhydride, when tertiary amine is used as a promoter, the cross-linking reaction between bisphenol A type epoxy resin and anhydride curing agent mainly involves the esterification reaction between epoxy groups and anhydride to form ester bonds[16]. The epoxy cross-linked network is mainly composed of epoxy segments and ester bond segments involved in the esterification reaction. Therefore, the epoxy/anhydride cross-linked network generated under the catalysis of tertiary amine can be deconstructed into two parts: epoxy segments and ester bond segments.

First, molecular models of epoxy segments and ester bond segments were established. As shown in Figure 1, these are the molecular models of epoxy segments and ester bond segments in the EP/MeTHPA cross-linked network. The epoxy segment refers to bisphenol A type epoxy molecules without epoxy groups at both ends, and the ester bond segment refers to the ester bond segment after ring-opening.

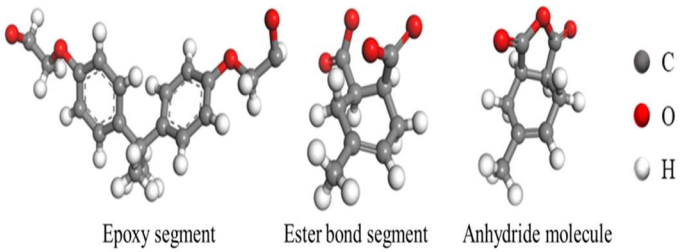


Figure. 1 Model of epoxy and anhydride segments in EP/MeTHPA cross-linked network

In the epoxy/anhydride cross-linked model, epoxy segments and ester bond segments were labeled. Due to the large scale of the molecular model, it was impossible for all anhydride molecules to participate in the cross-linking reaction through molecular dynamics methods, resulting in the presence of unreacted anhydride molecules in the cross-linked model. The distribution of epoxy segments, ester bond segments, and unreacted anhydride molecules in the EP/MeTHPA and EP/MeHHPA systems is shown in Figure 2.

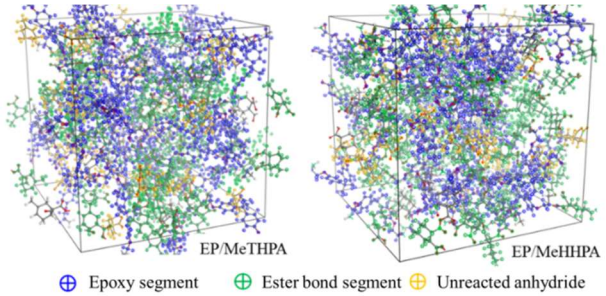


Figure. 2 Epoxy segments, ester bond segments and unreacted anhydride in epoxy cross-linked network

The quantities of epoxy segments, ester bond segments, and unreacted anhydride molecules in five different epoxy/anhydride systems were counted, as illustrated in Figure. 2, thereby deconstructing the epoxy/anhydride system. From Figure. 2, it is evident that epoxy segments and ester bond segments account for over 80% of the total segments in each epoxy/anhydride system, indicating that the cross-linking density in each system has reached 80%.

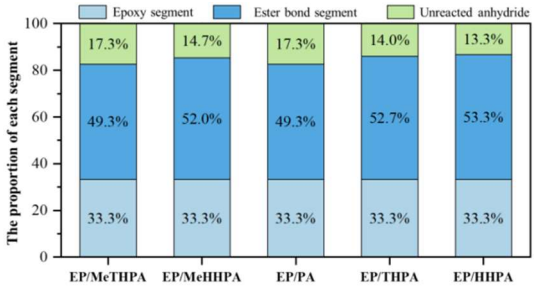


Figure. 3 The proportion of epoxy segments, ester bond segments and unreacted anhydride in different epoxy/anhydride molecular models

## 3. SEGMENTAL MOTION CHARACTERISTICS IN EPOXY/ANHYDRIDE CROSS-LINKED NETWORKS

To study the motion characteristics of each segment in the epoxy cross-linked network, the speed and displacement of the epoxy segments, ester bond segments, and unreacted anhydride segments in the deconstructed epoxy/anhydride cross-linked network were analyzed, clarifying the influence mechanism of the curing agent structure on the microscopic motion characteristics of the epoxy cross-linked network.

### 3.1 Velocity Distribution Patterns of Segments in Epoxy/Anhydride Cross-linked Networks

By traversing the cross-linked network, the position distribution and speed of specific segments in the epoxy/anhydride cross-linked network can be obtained. Figure 4 illustrates the position information and speed distribution of the ester bond segments in the EP/MeTHPA system.

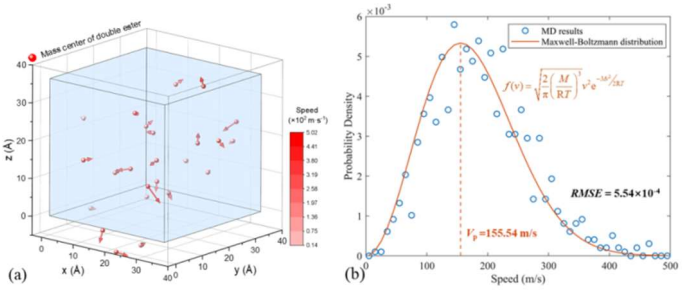


Figure. 4 Spatial distribution of ester bond segments (a) and speed probability distribution (b) in EP/MeTHPA cross-linked network

According to the curing reaction mechanism, the epoxy/anhydride cross-linked model was deconstructed into epoxy segments, ester bond segments, and unreacted anhydride segments. To further analyze the motion characteristics of each

segment in the cross-linked network, the speed of each segment in the epoxy/anhydride system under isothermal-isobaric ensemble (temperature 300 K, pressure 0.101 MPa) was extracted and fitted to the probability distribution of molecular motion speeds using the Maxwell-Boltzmann distribution, as shown in Eq (1).

$$f(v)=\sqrt{\frac{2}{\pi}\left(\frac{m}{kT}\right)^3}v^2\exp\left(\frac{-mv^2}{2kT}\right) \quad (1)$$

Where: $v$--particle motion speed/cm·s$^{-1}$; $m$-particle mass/g; $T$-temperature/K; $k$-Boltzmann constant.

The probability distribution and fitting results of segment motion speeds in the EP/MeTHPA cross-linked network at 300 K are shown in Figure 5. The fitting effect was evaluated using the root mean square error (RMSE). From Figure 5, it is evident that the probability density distribution of segment motion speeds in the epoxy cross-linked network conforms to the Maxwell-Boltzmann distribution. The derivative of Equation (1) with respect to speed yields the most probable speed $v_p$ of each segment, as expressed in Equation (2), with $v_p$ for each segment indicated in Figure 5.

$$v_p=\sqrt{2kT/m} \quad (2)$$

Where: $v_p$--most probable speed of particle motion/cm·s$^{-1}$.

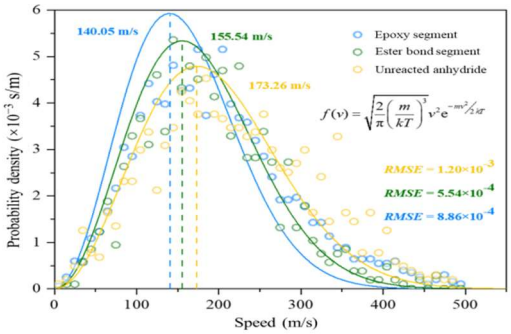


Figure. 5 Probability density distribution of segment speeds in EP/MeTHPA cross-linked system

### 3.2 Velocity Distribution Patterns of Segments in Epoxy/Anhydride Cross-linked Networks

According to dielectric relaxation theory, the $\beta$ dielectric relaxation of epoxy cured products at high frequencies is related to the motion of local chain segments in the cross-linked network. In previous studies, we proposed a method to optimize epoxy systems with low dielectric loss in high-frequency electric fields using mean squared displacement (MSD) as a surrogate measure. The definition of MSD is shown in the following equation:

$$\mathrm{MSD}=\frac{1}{N}\sum_{i=0}^{N-1}(|R_i(t)-R_i(0)|^2) \quad (3)$$

Where: $N$——number of atoms; $R_i(t)$——position of the $i$th atom at time $t$.

However, using the MSD of the entire cross-linked network as a surrogate measure makes it difficult to clarify the contributions of the motion of individual segments. Therefore, it is necessary to deconstruct the cross-linked network and analyze the contributions of each segment to the MSD of the epoxy/anhydride cross-linked network. According to the method mentioned in 2.1, five typical epoxy/anhydride systems (EP/PA, EP/THPA, EP/HHPA, EP/MeTHPA, and EP/MeHHPA) were deconstructed, and the displacement characteristics of each segment in the epoxy/anhydride systems were analyzed.

To clearly compare the mean squared displacement (MSD) of each segment in different epoxy/anhydride systems, the average MSD of each system's NPT ensemble from 100 to 200 ps was calculated to characterize the motion capabilities of each segment[17]. Figure 6 shows the mean squared displacement of each segment in different epoxy/anhydride cross-linked systems.

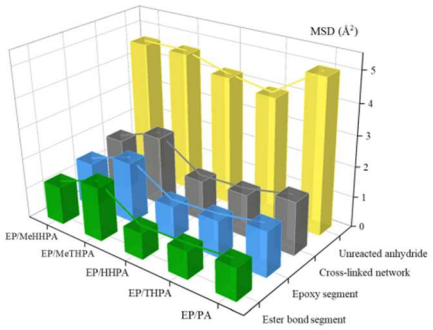


Figure. 6 Mean Squared Displacement of Each Segment in Different Epoxy Systems

The results indicate that within the epoxy/anhydride cross-linked network, the mean squared displacement of each segment generally adheres to the following order: unreacted anhydride >> epoxy segment > ester bond segment. Since the unreacted anhydride molecules are not bonded to the cross-linked network and are not restricted by it, they exhibit active motion capabilities, with mean squared displacement far greater than that of the segments within the cross-linked network. Conversely, once the anhydride molecules undergo esterification reactions with the epoxy resin, they become part of the cross-linked network, limiting their motion capabilities and significantly reducing their mean squared displacement.

Although the unreacted anhydride has strong mobility, its content in the epoxy/anhydride cross-linked network is low. In contrast, while the motion capabilities of epoxy segments and ester bond segments are weaker than those of unreacted anhydride molecules, they constitute the majority of the epoxy cross-linked system. Therefore, merely using the mean squared displacement to measure the average motion capabilities of atoms in different chain segments can only analyze the motion capabilities of the segments themselves and cannot analyze their contributions to the movement of the cross-linked network.

Consequently, the number of each segment in the five typical epoxy/anhydride systems mentioned above was tallied, and the displacement square of different segments in the epoxy cross-linked system was calculated based on the mean squared displacement of each segment, as shown in Equation (4), thus deconstructing the displacement characteristics of the cross-linked network into the displacement characteristics of each segment.

$$D^2 = \sum_{i=0}^{N-1} (|R_i(t) - R_i(0)|^2) \quad (4)$$

Where: $D$——displacement of a certain segment in the cross-linked network.

The displacement of the aforementioned five different epoxy/anhydride cross-linked systems was deconstructed into four parts: epoxy segments, ester bond segments, unreacted anhydride, and other atoms, as shown in Figure 7.

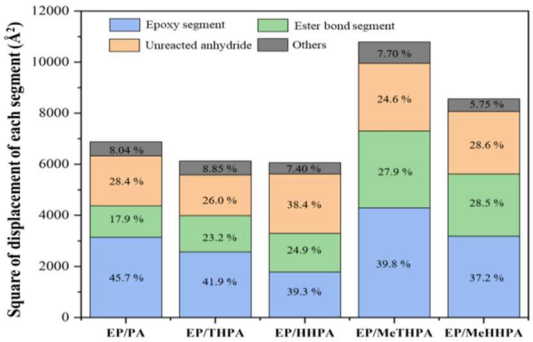


Figure. 7 Displacement Characteristics of Each Segment in Different Epoxy Systems

The results show that the displacement of epoxy segments, ester bond segments, and unreacted anhydride segments accounts for more than 90% of the total displacement, indicating the rationality of deconstructing the displacement of the epoxy/anhydride cross-linked system into epoxy segments, ester bond segments, and unreacted anhydride.

Comparing the displacement characteristics of segments in EP/PA, EP/THPA, and EP/HHPA systems reveals that the displacement capability of ester bond segments in the EP/PA system is lower than that in the EP/THPA and EP/HHPA systems; whereas the displacement capability of epoxy segments in the EP/PA system is higher than that in the EP/THPA and EP/HHPA systems.

This is attributed to the rigid saturated six-membered ring structure of PA, which reduces its mobility. The ester bonds formed by PA and epoxy resin also have rigidity, making their motion capability weaker compared to the ester bond segments in the EP/THPA and EP/HHPA systems. However, the rigid six-membered ring structure provides a "supporting" role for the cross-linked network, offering more free volume for the movement of epoxy segments, as shown in Figure 8. Therefore, compared to the EP/THPA and EP/HHPA systems, the epoxy segments in the EP/PA system have stronger motion capabilities and higher mean squared displacement.

Based on Figure 8, comparing the segment displacement characteristics of the EP/THPA and EP/HHPA systems with the EP/MeTHPA and EP/MeHHPA systems reveals that the overall displacement capability of the cross-linked network in the EP/MeTHPA and EP/MeHHPA systems is stronger than that in the EP/THPA and EP/HHPA systems.

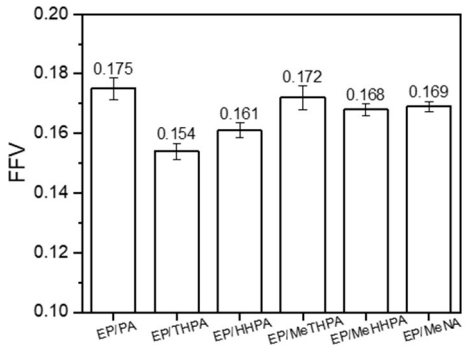


Figure. 8 Free Volume Fraction in Different Epoxy Systems

Compared to the EP/THPA and EP/HHPA systems, the anhydride in the EP/MeTHPA and EP/MeHHPA systems contains methyl side chains. The incorporation of methyl groups provides additional displacement to the ester bond segments. Furthermore, as shown in Figure 8, the free volume in the EP/MeTHPA and EP/MeHHPA systems is greater than that in the EP/THPA and EP/HHPA systems. Therefore, it can be concluded that the methyl groups play a "supporting" role in the cross-linked network, ultimately promoting the movement of the epoxy segments.

## 4. SUMMARY

The epoxy/anhydride cross-linked system was deconstructed into epoxy segments, anhydride segments, and unreacted anhydride segments, and the motion behavior of each local segment in the epoxy/anhydride cross-linked system was studied. The main conclusions are as follows:

(1) The probability density distribution of the motion speeds of epoxy segments, anhydride segments, and unreacted anhydride in the epoxy/anhydride cross-linked network conforms to the Maxwell-Boltzmann distribution.

(2) The increased rigidity of the six-membered ring in the curing agent reduces the displacement capability of anhydride and ester bond segments but provides a "supporting" role for the cross-linked network, thereby increasing the motion space of epoxy segments and reducing the motion resistance of epoxy segments.

(3) The methyl side chains in the anhydride provide additional displacement to the ester bond segments on one hand and also provide "support" to the cross-linked network on the other, thereby increasing the motion space of epoxy segments and reducing the motion resistance of epoxy segments.

## 5. REFERENCES

[1] Guillod T, Faerber R, Rothmund D, et al. Dielectric Losses in Dry-Type Insulation of Medium-Voltage Power Electronic Converters[J]. IEEE Journal of Emerging and Selected Topics in Power Electronics, 2020, 8(3): 2716-2732.

[2] Mishra DK, Ghadi MJ, Li L, et al. A review on solid-state transformer: A breakthrough technology for future smart distribution grids[J]. International Journal of Electrical Power & Energy Systems, 2021, 133: 107255.
[3] Awais M, Chen X, Dai C, et al. Tuning Epoxy for Medium Frequency Transformer Application: Resin Optimization and Characterization of Nanocomposites at High Temperature[J]. IEEE Transactions on Dielectrics and Electrical Insulation, 2021, 28(5): 1751-1758.
[4] Adhikari P, Ghassemi M. A Comprehensive Review of Mitigation Strategies to Address Insulation Challenges within High Voltage, High Power Density (U)WBG Power Module Packages[J]. IEEE Transactions on Dielectrics and Electrical Insulation, 2024: 1-1.
[5] Zahidul Islam M, Fu Y, Deb H, et al. Polymer-based low dielectric constant and loss materials for high-speed communication network: Dielectric constants and challenges[J]. European Polymer Journal, 2023, 200: 112543.
[6] Lokanathan M, Acharya PV, Ouroua A, et al. Review of Nanocomposite Dielectric Materials With High Thermal Conductivity[J]. Proceedings of the IEEE, 2021, 109(8): 1364-1397.
[7] Liu J, Wu M, Fu Z, et al. Enhancing flame retardancy and dielectric performance of epoxy resins through benzoxazine-phosphorus modification[J]. Polymer, 2024, 305: 127173.
[8] Bai L, Xu R, Wu W, et al. Insights into adsorbent materials for lithium extraction by capacitive deionization: reconceptualizing the role of materials informatics[J]. J. Mater. Chem. A, 2024, 12(18): 10676-10685.
[9] Kozinsky B, Singh DJ. Thermoelectrics by Computational Design: Progress and Opportunities[J]. Annual Review of Materials Research, 2021, 51(Volume 51, 2021): 565-590.
[10] Hippalgaonkar K, Li Q, Wang X, et al. Knowledge-integrated machine learning for materials: lessons from gameplaying and robotics[J]. Nat Rev Mater, 2023, 8(4): 241-260.
[11] Shang X, Pang L, Bu Q, et al. Thermal runaway and induced electrical failure of epoxy resin in high-frequency transformers: Insulation design reference[J]. High Voltage, 2024, n/a(n/a).
[12] Wu Z, Lin B, Fan J, et al. Effect of Dielectric Relaxation of Epoxy Resin on Dielectric Loss of Medium-Frequency Transformer[J]. IEEE Trans. Dielect. Electr. Insul., 2022, 29(5): 1651-1658.
[13] Khodadadi A, Haghighi M, Golestanian H, et al. Molecular Dynamics Simulation of Functional and Hybrid Epoxy Based Nanocomposites[J]. Mechanics of Advanced Composite Structures, 2020, 7(2): 233-243.
[14] Yang Y, Ma J, Yang J, et al. Molecular Dynamics Simulation on In-Plane Thermal Conductivity of Graphene/Hexagonal Boron Nitride van der Waals Heterostructures[J]. ACS Appl. Mater. Interfaces, 2022, 14(40): 45742-45751.
[15] Wang L, Yang J, Cheng W, et al. Progress on Polymer Composites With Low Dielectric Constant and Low Dielectric Loss for High-Frequency Signal Transmission[J]. Front. Mater., 2021, 8.
[16] Li J, Aung HH, Du B. Curing Regime-Modulating Insulation Performance of Anhydride-Cured Epoxy Resin: A Review[J]. Molecules, 2023, 28(2): 547.
[17] Wu Z, Fan J, Zhao Y, et al. Computationally driven design of low dielectric-loss epoxy resin for medium-frequency transformers[J]. J. Phys. D: Appl. Phys., 2023, 56(18): 184001.